Microphone array method for the characterization of rotating sound sources in axial fans[1)]

Gert Herold[a)] and Ennes Sarradj[b)]

(Received: 7 July 2015; Revised: 24 November 2015; Accepted: 24 November 2015)

Methods based on microphone array measurements provide a powerful tool for determining the location and magnitude of acoustic sources. For stationary sources, sophisticated algorithms working in the frequency domain can be applied. By using circularly arranged arrays and interpolating between microphone signals it is possible to treat rotating sources, as are present in fans, as being non-moving. Measurements conducted with a four-bladed fan and analyzed with the "virtual rotating array" method show that it is not only possible to identify the main noise contributors, but also to determine a full spectrum for any rotating component of interest. © *2015 Institute of Noise Control Engineering.*

Primary subject classification: 74.6; Secondary subject classification: 11.4.1

1 INTRODUCTION

Microphone arrays as tools for characterizing acoustic sources have become state of the art in many fields of application. The principle behind the widely used beamforming algorithms is to shift the measured time signals to compensate the sound travel time from a chosen "focus" point to each of the microphones. If the focus point contains a source, a summation of the signals will reveal a maximum; otherwise the signals mostly cancel each other out[1].

Beamforming can be done in time domain and in frequency domain. In time domain, the signals are directly delayed and summed. In frequency domain, the signals are first Fourier-transformed and their cross-spectra are averaged. A multiplication of the resulting complex cross-spectral matrix (CSM) with steering vectors fulfills the task of phase-shifting the signals according to the focus points and subsequent summation. The direct averaging of the cross-spectra has the advantage that non-continuous sources are canceled out before the actual beamforming. Furthermore, uncorrelated background noise can be accounted for via removal of the main diagonal of the CSM.

In the case of moving sources, usually a time domain formulation is used, since the distances from focus points to microphones constantly change and this time-depending phase-shift cannot be taken into account with pre-averaged data, as is the case in frequency domain. The application of time domain beamforming on rotating sources was presented by Sijtsma et al.[2] and Minck et al.[3]. Because of the need for oversampling and the necessity to continuously recalculate distances and interpolate the signal samples accordingly, the time domain beamforming on moving sources is rather time-consuming in comparison to frequency domain beamforming on stationary sources. On the other hand, frequency domain beamforming is based on the measured CSM, which makes it possible for more sophisticated high-resolution source characterization methods, such as CLEAN-SC[4], to be applied. Therefore, in terms of computational handling, it would be beneficial to move the microphones parallel to the trajectory of the moving sound sources to be able to regard them as stationary in the moving reference system. This is usually not physically practicable.

However, in the case of rotating sources, such as occur in fans, it is possible to take advantage of rotational symmetry if the signals are measured with a circular, axially centered array. Lowis and Joseph[5] used a Green's function that takes into account source rotation to detect rotating sources in ducts with near-field acoustic holography. A similar approach has been followed for the prediction of tonal noise in axial fans[6]. Pannert and Maier[7] adapted the model to free-field conditions and applied the method to inversely determine a CSM in the rotating reference system from a CSM calculated from signals measured at fixed positions. In order to make this Green's function applicable, however, a uniform rotation with a

[1)] This is the third paper published in NCEJ on the special topic of Fan Noise.

[a)] Brandenburg University of Technology, Technical Acoustics, Siemens-Halske-Ring 14, D-03046 Cottbus, GERMANY; email: gert.herold@b-tu.de.

[b)] Brandenburg University of Technology, Technical Acoustics, Siemens-Halske-Ring 14, D-03046 Cottbus, GERMANY; email: ennes.sarradj@b-tu.de.

constant angular frequency has to be assumed. As this is not a reasonable assumption when conducting measurements on actual fans, a different approach is pursued here. Enhancing the technique proposed by Dougherty and Walker[8], a virtual rotating array is approximated through interpolation of the measured signals according to the momentary angular position of the measured object.

The remainder of this paper is organized as follows. In the theory section a short summary of frequency domain beamforming including CLEAN-SC deconvolution is given and the principle of the virtual rotating array is explained. The setup section features a description of the conducted experiment with a four-bladed fan and a circular microphone array. Then the obtained results are presented and discussed. Finally, the findings are summarized in the concluding section.

2 THEORY

2.1 Beamforming and CLEAN-SC

Considering a grid of N focus points $\boldsymbol{x}_t$, the frequency domain formulation for the basic delay-and-sum beamformer is

$$B(\boldsymbol{x}_t) = \boldsymbol{h}^{\mathrm{H}}(\boldsymbol{x}_t)\, \boldsymbol{C}\, \boldsymbol{h}(\boldsymbol{x}_t)\,, \quad t = 1 \ldots N, \tag{1}$$

with the superscript $^{\mathrm{H}}$ denoting the Hermitian transpose. The steering vector $\boldsymbol{h}$, which has as many entries as number of microphones M used, comprises the phase shift and amplitude correction to "steer" the array to a focus point:

$$h_m = \frac{1}{r_{t,m}\sqrt{M\sum_{l=1}^{M} r_{t,l}{}^{-2}}} e^{-\mathrm{j}k(r_{t,m}-r_{t,0})}, \quad m = 1 \ldots M. \tag{2}$$

This corresponds to formulation IV in Ref. 9. $\boldsymbol{C}$ is an approximation of the CSM and is obtained by averaging the cross-spectra. These are calculated from the windowed and FFT-transformed time signals, which are measured by the microphones. Since the auto-spectra do not contain any information about phase differences between the signals or any information about the amplitudes that is not implicitly present in other matrix entries, the main diagonal of $\boldsymbol{C}$ can be left out from the analysis to reduce errors introduced by uncorrelated background noise from the measurements.

The beamformer output $B(\boldsymbol{x}_\mathrm{t})$ can be interpreted as the actual source distribution convoluted with a point spread function, i.e., the properties of the beamforming algorithm, together with the chosen microphone array geometry, introduce a systematic error that leads to a rather blurred sound map.

To overcome this problem, several methods have been proposed, with CLEAN-SC[3] being one of the fastest algorithms. Its basic working principle is that the algorithm searches for the highest peak in the beamformer output and copies its value into an initially empty (clean) map. It then identifies coherent portions and subtracts them from the original (dirty) map, leaving a different maximum. This process is then reiterated until no more significant sources are found in the dirty map or a maximum number of iterations is reached.

2.2 Virtual Rotating Array

The working principle of the presented method is to determine the sound pressures at the positions of a virtual microphone array which is rotating at the exact same rate as the measured object. These virtual signals are based directly on the physically measured sound pressures at the fixed microphone positions for each time sample. Most of the time, this virtual rotating array includes positions where no actual microphones are installed. The sound pressures at these positions are therefore linearly interpolated between measured sound pressures at neighboring actual microphones.

Let M be the number of microphones arranged regularly in one ring and $p_m(t)$ the measured sound pressures ($m = 1 \ldots M$). The angle between each microphone can then be calculated by:

$$\alpha = \frac{2\pi}{M}\,. \tag{3}$$

With the time-dependent angle of the measured object $\varphi(t)$, the lower and upper indices of the microphone signals between which to interpolate can be calculated via:

$$\begin{aligned} m_1(m,t) &= \left\lfloor m + \frac{\varphi(t)}{\alpha} - 1 \right\rfloor \bmod M + 1 \\ m_u(m,t) &= \left\lfloor m + \frac{\varphi(t)}{\alpha} \right\rfloor \bmod M + 1, \end{aligned} \tag{4}$$

with $\lfloor \cdot \rfloor$ denoting the floor function. The weighting factors for the respective sound pressures are:

$$\begin{aligned} s_\mathrm{u}(t) &= \frac{\varphi(t)}{\alpha} - \left\lfloor \frac{\varphi(t)}{\alpha} \right\rfloor \\ s_\mathrm{l}(t) &= 1 - s_\mathrm{u}(t)\,. \end{aligned} \tag{5}$$

Finally, the microphone signals of the virtual rotating array can be calculated:

$$p_{\mathrm{vr},m}(t) = s_\mathrm{l} p_{m_\mathrm{l}} + s_\mathrm{u} p_{m_\mathrm{u}}. \tag{6}$$

As can be seen from Eqn. (5), in case of the current angle $\varphi(t)$ being an integer multiple of the angle between the microphones α, s_u becomes zero, and an actually measured (non-interpolated) sound pressure is evaluated.

With this formulation, the virtual array can be kept synchronized with the rotation of any object on the same rotational axis, provided the angular movement

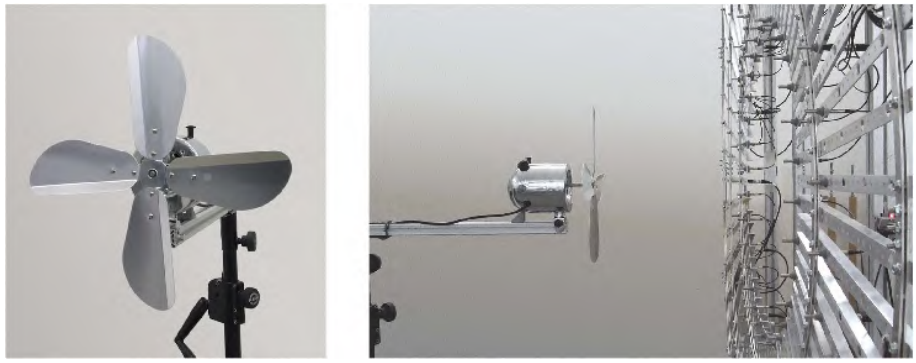

Fig. 1—Fan used for the measurements. Fan with microphone array (only the inner ring of microphones was used).

of that object $\varphi(t)$ is logged with sufficient detail. The CSM for the virtual rotating array is calculated equivalently to the stationary case.

It should be kept in mind that, when using a rotating array (physical or virtual), the medium between microphones and sources usually does not rotate with the same angular velocity and therefore in the rotating reference system is not resting, but rotating itself. For the application of beamforming, a sufficiently precise model of the retarded times, i.e., the sound travel times between assumed source positions and microphones, is necessary, and ignoring the rotating medium will lead to inaccurate results. However, to calculate the retarded times for each sample with an arbitrarily changing angle $\varphi(t)$ is computationally very costly, as this cannot be done analytically. For the purpose of this paper, therefore, it is assumed that the angular velocity changes little enough for the retarded times to be considered constant and calculated with sufficient precision using the mean angular velocity.

The virtual rotating array method can easily be extended for the use of several rings of microphones if necessary. As is shown in this contribution, results obtained with only one ring are already acceptable.

3 SETUP

Measurements were performed on a four-bladed common household fan with a diameter of 0.4 m. The fan was primarily chosen for its distinctive and simple geometry as well as its noisiness rather than its aerodynamic efficiency. The blades consist of flat metal sheets with slanted trailing edges.

Table 1—Measurement and data processing parameters.

Number of microphones	32
Diameter of ring array	0.8 m
Distance from fan to array	0.4 m
Sampling rate	51.2 kHz
FFT block size	4096 samples
FFT window	von Hann, 50% overlap
Resolution of focus grid	0.01 m
CLEAN-SC iterations	500

The microphone array consists of 32 microphones arranged circularly in one ring, which was positioned parallel to the fan (see Fig. 1). Important measurement and data processing parameters are summarized in Table 1. Three operating cases of the clock-wise rotating fan were evaluated for this paper:

- the fan rotating at 1315 rpm,
- the fan at 1150 rpm with an applied obstruction on one blade (see Fig. 2),
- the backwards mounted fan (trailing edge as leading edge) at 1366 rpm.

The flow direction was towards the microphone array, except for reversed installation, where the direction

Fig. 2—Fan with applied flow obstruction (ball type cable tie) at the trailing edge of the blade at 6 o'clock.

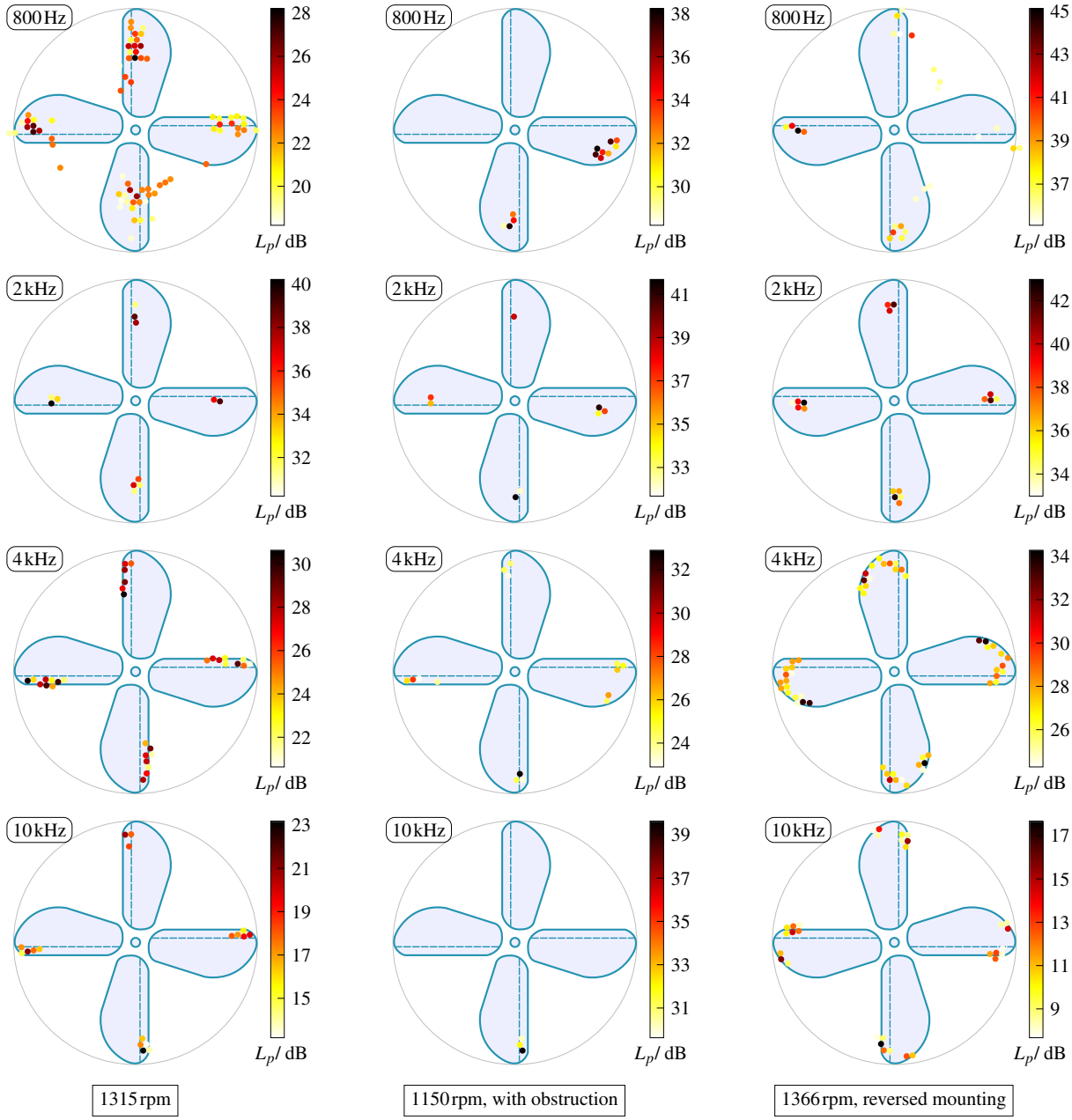

Fig. 3—CLEAN-SC sound maps for a clock-wise rotating fan using the virtual rotating array method. The results of three different measurement cases (columns) are evaluated at exemplary one-third octave bands (rows). Displayed are reconstructed sound pressure levels up to 10 dB below the respective band maximum level.

of the generated flow was not very distinct. Other than the mounting of the fan, there were no obstacles in the flow. The array itself is constructed in such a way that the flow can pass through its center without disturbance. No acoustic absorbers were used, but since the fan axis is 1.5 m above the ground and the experiments were conducted in a hall approximately 6 m high, the influence of reflections can be neglected. No measurements to evaluate the aerodynamic characteristics of the fan have been performed, as this would be beyond the scope of this paper.

In order to track the rotational movement of the fan, a laser reflector was applied to one fan blade, so that one trigger could be logged per revolution. The trigger signal was recorded simultaneously along with the microphone signals. The angles corresponding to each sample were calculated in post-processing using a spline interpolation of the known positions at the trigger instants.

4 RESULTS

Sound pressures were calculated on a cylindrical grid, enveloping the fan with an extension of the grid

in axis direction of 0.04 m. The grid points are evenly distributed, with a resolution of 0.01 m. For display, the values were summed in axis-direction. Sound maps for the three measured cases are shown in Fig. 3. Each map shows the reconstructed sound pressure levels at the focus points, evaluated for a one-third octave band with the designated band center frequency, in a 10 dB range including the occurring maximum level.

It has to be noted that it is intrinsic to the applied CLEAN-SC deconvolution algorithm to assign correlated sources to a single focus point, without taking into account the extent of the actual source. Therefore, coherent sources that are in fact distributed over an area discretized by several points are artificially "condensed." In particular, sources at low frequencies, whose extent exceeds the area described by a single focus point, are nevertheless found only at one position. This has to be kept in mind when evaluating the sound maps.

In case of the fan rotating at 1315 rpm, the maps indicate that for higher frequencies the main sources are more and more found towards the trailing edge and the tip of the blades, where the turbulent separation at the sharp trailing edge seems to be the dominant noise generating mechanism. At 4000 Hz, the main source region spans about half the trailing edge of the blades. At 2000 Hz and below, the major sources are detected on the broadest part of the blade.

With the cable tie applied on the lowermost blade's trailing edge (center column in Fig. 3), noise is generated not only at the disturbed blade, but also at the following blade. The fact that this phenomenon is most distinctive at the 800 Hz band suggests that mostly larger turbulent structures caused by the flow obstruction interact with the leading edge of the following blade.

When mounting the blades facing the wrong way, the flow detaches at the (non-intended) leading edge, generating noise at the outer leading and trailing edges (best visible at 4000 and 10,000 Hz).

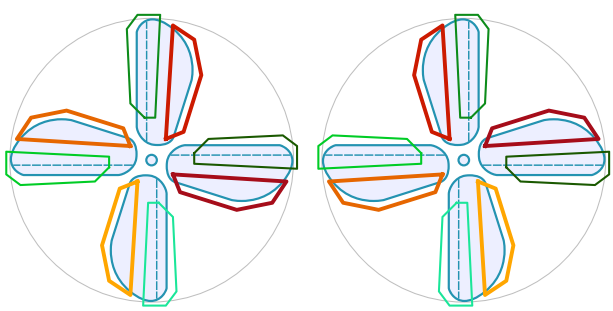

Fig. 4—Schematic of the fan with assigned integration sectors (left: normal mounting, right: reversed mounting). Shades of red: leading edges, shades of green: trailing edges.

In order to quantitatively evaluate the emitted noise spectra at the leading and trailing edges, the calculated sound pressures at locations inside the according areas, indicated by the red and green polygons in Fig. 4, were summed for each frequency band.

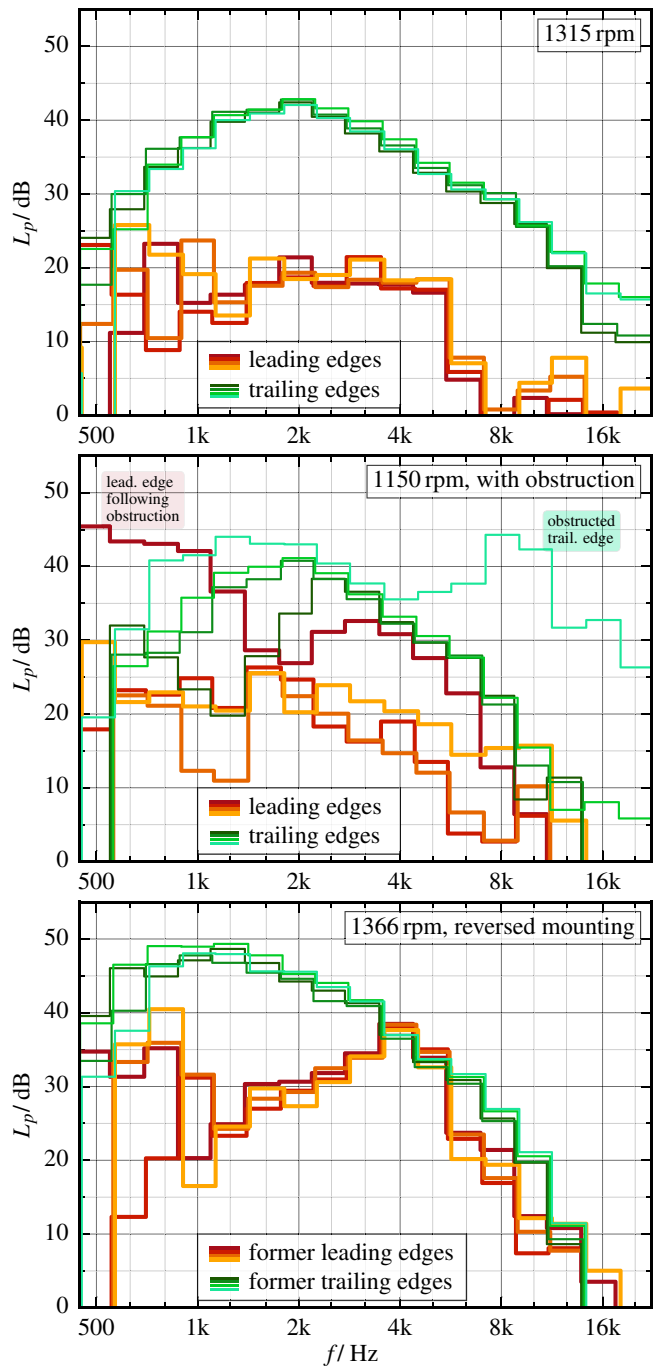

Fig. 5—Leading and trailing edge spectra (sound pressure level) for the fan at different operating cases. In the case of the backwards mounted fan, the slanted parts of the blades are facing the flow, i.e., the former trailing edge is in fact leading edge and vice versa.

Figure 5 shows the integrated spectra for the measured cases. The bold lines in red shades and the thin lines in green shades represent the spectra at the corresponding bordered areas shown in Fig. 3. The respective shades get "lighter" in anti-clockwise direction, starting with the 3-o'clock blade.

For the pure fan, rotating at 1315 rpm, all blades show approximately the same spectra, with more variation at the leading edges below 1000 Hz. It can be seen that the sound pressure levels at the trailing edges are always higher than those at the leading edges, which confirms the former to be the main source of noise radiation. The spectrum at the trailing edge is also rather broadband, with a not very sharp maximum at 2000 Hz.

When applying the flow obstruction, the spectra paint a different picture. The trailing edge of the 6-o'clock blade (light green curve) radiates at higher levels than all other blades, especially above 4000 Hz. On the other hand, the leading edge of the subsequent 3-o'clock blade (dark red) is rather loud in comparison to the other blades as well, even exceeding the level of the disturbed trailing edge at 1000 Hz and below.

For the measurements of the reversely mounted fan, the slanted portions of the blade are the actual leading edges. The integrated spectra show that those play the dominant role in noise generation. Furthermore, the overall noise emission, in particular at frequencies below 5000 Hz, is much higher than in case of the correctly mounted fan.

5 CONCLUSION

A method for the assessment of rotating sources has been presented. The algorithm calculates interpolated sound pressures based on the synchronized rotation of a virtual array. This procedure allows the application of sophisticated source characterization methods that are otherwise only available for stationary sources.

The virtual rotating array method has been successfully tested on a common household fan in different configurations. Even though the existing flow field was not taken into account for this analysis, the presented results allow drawing deductions concerning the occurring source mechanisms.

6 REFERENCES

1. D.H. Johnson and D.E. Dudgeon, *Array Signal Processing, Concepts and Techniques*, P T R Prentice Hall, Englewood Cliffs, (1993).
2. P. Sijtsma, S. Oerlemans and H. Holthusen, "Location of rotating sources by phased array measurements", *7th AIAA/CEAS Aeroacoustics Conference*, (2001).
3. O. Minck, N. Binder, O. Cherrier, L. Lamotte and V. Budinger, "Fan noise analysis using a micro-phone array", *Fan 2012 — International Conference on Fan Noise*, (2012).
4. P. Sijtsma, "CLEAN based on spatial source coherence", *International Journal of Aeroacoustics*, **6**(4), 357–374, (2007).
5. C.R. Lowis and P.F. Joseph, "Determining the strength of rotating broadband sources in ducts by inverse methods", *J. Sound Vibr.*, **295**(3–5), 614–632, (2006).
6. A. Gérard, A. Berry and P. Masson, "Control of tonal noise from subsonic axial fan, Part 1", *J. Sound Vibr.*, **288**(4–5), 1049–1075, (2005).
7. W. Pannert and C. Maier, "Rotating beamforming — motion-compensation in the frequency domain and application of high-resolution beamforming algorithms", *J. Sound Vibr.*, **333**(7), 1899–1912, (2014).
8. R.P. Dougherty and B.E. Walker, "Virtual rotating microphone imaging of broadband fan noise", *15th AIAA/CEAS Aeroacoustics Conference*, (2009).
9. E. Sarradj, "Three-dimensional acoustic source mapping with different beamforming steering vector formulations", *Advances in Acoustics and Vibration*, **2012**, 1–12, (2012).